

EDGE ENHANCED SPATIO-TEMPORAL CONSTRAINED RECONSTRUCTION OF UNDERSAMPLED DYNAMIC CONTRAST ENHANCED RADIAL MRI

Srikant K. Iyer^{1,2,3}, Edward V.R DiBella^{3,4}, Tolga Tasdizen^{1,2}

¹Electrical and Computer Engineering department, ²SCI Institute, School of Computing, ³UCAIR, Department of Radiology, ⁴Department of Bioengineering, University of Utah, Salt Lake City, Utah, USA

ABSTRACT

There are many applications in MRI where it is desirable to have high spatial and high temporal resolution. This can be achieved by undersampling of k-space and requires special techniques for reconstruction. Even if undersampling artifacts are removed, sharpness of the edges can be a problem. We propose a new technique that uses the gradient from a reference image to improve the quality of the edges in the reconstructed image along with a spatio-temporal constraint to reduce aliasing artifacts and noise. The reference is created from undersampled dynamic data by combining several adjacent frames. The method was tested on undersampled radial DCE MRI data with little respiratory motion. The proposed method was compared to reconstruction using the spatio-temporal constrained reconstruction. Sharper edges and an increase in the contrast was observed by using the proposed method.

Index Terms— DCE MRI, reconstruction, regularization, PDE.

1. INTRODUCTION

Dynamic Contrast Enhanced (DCE) MRI is used to track changes in an organ or area of interest over time. A contrast agent is injected and a series of k-space data is acquired over time. Spatio-temporal resolution is limited since relatively rapid tracking of the contrast agent is necessary. Improved resolution is possible from undersampled k-space data, although this results in artifacts in accordance with Shannon/Nyquist sampling theorem. When some prior information about the image is available and appropriately incorporated into the reconstruction, accurate reconstruction may still be possible even when the sampling theorem is violated.

Methods such as keyhole imaging [1,2] and reduced-encoding MRI imaging with generalized-series reconstruction (RIGR) [3-4] assume that in a dynamic sequence of images the high frequency data remains static while only the low frequency data changes. Hence only low frequency data is acquired rapidly once a completely sampled k-space frame has been acquired. However, in most cases, the assumption about static high frequency content is not accurate. Other methods like highly constrained back projection reconstruction (HYPR) [5] use a composite image to improve the sharpness of the edges in the reconstructed image. Recently a Temporally Constrained Reconstruction (TCR) [6] and subsequently a Spatio-Temporal Constrained Reconstruction (STCR) [7,8] was proposed to reconstruct sparse myocardial perfusion data with some respiratory motion. We propose to extend the STCR method [7,8] to achieve sharper edges by incorporating an edge enhancement function based on a reference image. The new method is termed Edge Enhanced Spatio-Temporal Constrained Reconstruction (EESTCR). We demonstrate the method on simulated and acquired radial k-space data.

2. METHODS

2.1 Theory

Artifacts that occur due to reconstruction from sparse k-space data can be removed by using a priori information about the fully sampled data incorporated as constraints into a regularization framework as defined in [6,7,8]. Here the cost function is extended to handle the spatial regularization by minimizing the cost function C given by

$$\min_m(C) = \min_m(\phi + \alpha_1 T + \alpha_2(1 - \omega)S + \alpha_3 \omega E) \quad (1)$$

where \tilde{m} represents the estimated complex image data, ϕ is the fidelity to the acquired sparse data, T the temporal constraint and S and E represent the spatial gradient constraint and the proposed edge constraint, respectively. The fidelity term is given by $\phi = \|WF\tilde{m} - \tilde{d}\|_2^2$ where $\|\cdot\|_2$ represents the L_2 norm, F is the Fourier transform operator, W is the binary sparsifying pattern used to obtain the sparse data from full data, and \tilde{d} is the acquired sparse k-space data. The temporal regularization term is a total variation in time penalty [8] given by $T = \sum_{i=1}^N \|\nabla_t \tilde{m}_i\|$ where ∇_t is the temporal

gradient operator and N is the total number of pixels in each time frame and m_i represents the time curve of pixel i . The spatial regularization term S is a spatial total variation (TV) penalty [7,8] given by $S = \sum_{j=1}^M \left\| \sqrt{\nabla_x \tilde{m}_j^2 + \nabla_y \tilde{m}_j^2 + \beta^2} \right\|$ where $\|\cdot\|_1$ represents the L1

norm, M the total number of time frames, ∇_x and ∇_y represent the spatial gradients along x and y direction respectively and β is a small positive constant on the order of machine precision [7,8]. To improve the sharpness of the edges we propose to add the edge constraint given by $E = \|\nabla_{xy} \tilde{m} - \nabla_{xy} I_r\|_1$ where I_r is the reference image, ∇_{xy} is the spatial gradient, and ω is a spatially varying weight defined as $\omega = 1 - \exp(-|\nabla_r^2 I_r| / \lambda^2)$, λ is a constant. α_1, α_2 and α_3 are weights that control the amount of spatial TV regularization, temporal regularization and the gradient matching term respectively.

The term $\|\nabla_{xy} \tilde{m} - \nabla_{xy} I_r\|_1$ is used to match the gradients of the reconstructed image and the gradients of the reference image that correspond to edges. The function ω is used to form a map of the strength of the edges in the reference image. The term $(1-\omega)$ is used to control the influence of the TV minimization at areas where the gradient of the reference image is very large. At such points, the value of ω is close to 1 and hence $(1-\omega)$ is almost zero. This prevents the influence of TV minimization at sharp edges

where only the edge matching function would take effect, avoiding smoothing of edges due to spatial regularization. This leads to improvement of the sharpness of the edges by the edge constraint and at the same time the streaking and noise are removed by the spatial and temporal regularization terms. Reconstruction is performed by minimizing the cost function, C , given by

$$C = \|WF\tilde{m} - \tilde{d}\|_2^2 + \alpha_1 \sum_{j=1}^N \|\nabla_x \tilde{m}_j\| + \alpha_2 (1 - \omega) \sum_{j=1}^M \left\| \sqrt{\nabla_x \tilde{m}_j^2 + \nabla_y \tilde{m}_j^2 + \beta^2} \right\| + \alpha_3 \omega \|\nabla_x \tilde{m} - \nabla_x I_r\|_1 \quad (2)$$

Here the reference frame I_r is created from the undersampled dynamic data. Several adjacent frames are combined as described below to obtain a fully sampled image with enough edge information to be utilized by the edge enhancement function.

2.2. Myocardial perfusion data

The method was first tested on radial data simulated from full k-space Cartesian data. Only the spatial term, fidelity term and edge enhancement term (without temporal constraint) were used in order to study the effects of the edge enhancement function. This simulation helped in understanding the edge enhancement function better. The method was also tested on acquired undersampled radial data with all four constraints (fidelity, spatial, temporal and edge constraint). Both Cartesian and radial data perfusion data were obtained from a Siemens Trio 3T scanner with a phased array cardiac coil. For both Cartesian and radial data, a saturation recovery turbo flash sequence with TR/TE~(2.5/1.4) msec, with a 12 degree flip angle, and 8 mm slice thickness was used.

To simulate the undersampled radial acquisition from the Cartesian data, 24 equiangular rays were created from the Cartesian samples. Edge enhanced spatially constrained reconstruction (EESCR) was performed on the simulated radial data by setting α_1 to zero and choosing α_2 and α_3 empirically to give good image quality. The choice of λ was based on the edge map from the reference image itself i.e. by looking at ω as shown in Figure 1. A λ value that appeared to give the sharpest edges was used. Full k-space data for the reference image was created by using 96 equi-angular radial lines from the Cartesian data using a binary mask. 96 lines were chosen because the IFT closely matched that of the full k-space data [7]. The binary mask used to simulate undersampled radial data was rotated by a random angle for different time frames.

For the acquired 24 ray radial data case, fully sampled data for the reference frame was created from the last 4 time frames. The acquisition used a start angle offset of $180/96^\circ$ that repeated every four frames, so that a combination of four frames gave 96 unique equiangular rays. The parameters for EESTCR were chosen based on the results from a training dataset. The regularization weights were chosen as $\alpha_1=0.05$, $\alpha_2=0.005$, and $\alpha_3=0.05$. The step size for the gradient descent was fixed at 0.05 and 150 iterations were performed to minimize the cost function C . For the edge function ω , the value of λ was chosen as $\lambda=0.02$. As discussed in [7,8] the regularization weights were robust to slight perturbations. We found that for a given type of acquisition and undersampling the values of α_1 , α_2 , α_3 and λ did not change significantly.

3. RESULTS

3.1. Edge Enhanced Spatially Constrained Reconstruction (EESCR) using simulated radial data

The reference image, the IFT of the simulated under-sampled radial data, the edge function ω , and the reconstructed image using EESCR are shown in Fig 2. As seen in the IFT, because the higher frequencies have been undersampled the most, the edges appear smooth. The edge enhancement function seeks to improve the quality of these smooth edges by making them sharper using the edge function and the edge map. A comparison between the IFT and the EESCR image shows that the EESCR image has much sharper edges. Since EESCR uses no temporal constraint, each reconstructed frame is independent of the others and has low computational cost relative to reconstructing all of the frames simultaneously.

3.2. Edge enhanced spatio-temporal constrained reconstruction (EESTCR) using acquired radial data

When reconstructing undersampled radial data, including a temporal constraint was considered necessary as a temporal constraint performs much better than a spatial constraint for undersampled data [7,8]. Reconstructed images using IFT, STCR and EESTCR are shown in figure 3. Improvement in the sharpness of edges was seen in the reconstructed images by using EESTCR. Only edges that were present in the edge map were enhanced using the proposed edge function. EESTCR was more robust to motion than EESCR. Even when there was respiratory motion, improvement in the sharpness of edges was still seen as shown in Figure 3d and Figure 3e. The difference image (Figure 3d) between EESTCR and STCR shows that the edges were enhanced using EESTCR as compared to STCR. Edges in the vessels in the lungs, myocardium and papillary muscles were also more clear. The line profiles of IFT, STCR and EESTCR were shown in figure 3e and figure 3f. The peaks in the line profile of EESTCR are higher and the valleys are lower in comparison with STCR. In some reconstruction a faint edge was seen in a couple of initial frames before there was any contrast in the LV. This was not considered a problem as we are only interested in frames after the onset of contrast in the LV, and after the onset of contrast in the LV no such false edges are seen.

The mean intensity curves of STCR and EESTCR are shown in figure 4 and are similar. In some cases when the reference image formed by combining the last 4 frames did not contain much edge information, only slight improvement over STCR was seen. This shows that a good reference image with sufficient edge information is necessary for the edge enhancement function to function properly. However, a poor reference image did not degrade the image quality beyond that of STCR. To address the problem of sub-optimal reference images, we also tried combining 4 frames from the middle of the sequence where there was better contrast in the LV to get the reference frame. Using this reference frame, an improvement in the sharpness of the edges was seen when compared with using the reference frame towards the end of the dynamic series. The results are shown in figure 5. The line profiles in figure 5d show that EESTCR with reference frame constructed by combining 4 frames from the centre of the dynamic sequence could make some more improvement in the sharpness of edges. As the contrast was better in images from centre of the dynamic sequence, a reference frame formed by combining them had better edge information and hence edge map ω and the

gradients matching term were able to map and reconstruct the edge information better.

4. DISCUSSION

We presented a gradient matching term based edge enhancement function in conjunction with STCR. Although the method was tested with dynamic cardiac perfusion data, it is equally applicable to other DCE MRI studies such as breast or brain tumors with undersampled data. Since there are less motion problems in brain and breast studies, the edge enhancement function would likely perform better as there will be little or no edge mismatch between the reconstructed and reference images. This would in turn allow for much higher undersampling factors. With a fully sampled reference frame and no edge mismatch between the undersampled frames, reconstructing with EESTCR would produce reconstructions with sharper edges while high temporal resolution would also be achieved due to higher sparsification factors.

Dynamic myocardial perfusion images are often used to estimate the kinetic parameters using the change in intensity curves to fit a pharmacokinetic model. Registration and segmentation are two key areas that using EESTCR would be useful. Any improvement in the sharpness of edges would improve manual or automatic segmentation of the endocardial and epicardial borders of the LV and also could aid in the registration process. Providing even slightly sharper edges in the reconstructed images would help reduce intra-user variability in image registration and segmentation.

The method was tested using a single reference frame. A fully sampled reference image was created by combining multiple interleaved frames. This is a limitation of this study as the fully sampled reference frame was not actually acquired. But this

limitation is not significant as towards the end of the acquisition the contrast varies slowly and images formed by combining multiple undersampled frames would be similar to a single fully sampled frame. Using a multiple reference image EESTCR method would be more tolerant to motion.

Although not shown here, it was also seen that an edge mismatch between the reference image and the reconstructed images due to Cartesian respiratory motion lead to a faint false edge being created in the reconstructed frame. To overcome this problem in EESCR, the reference frame was updated after each frame was reconstructed. The last frame 'n' was reconstructed first and this reconstructed frame was used as reference frame to reconstruct frame 'n-1' and so on. Hence each reconstructed frame was used as reference frame for the previous frame. This made the reconstructions more tolerant to motion in this case, though was not employed in the acquired radial data shown here. Using a multiple reference image EESTCR method might be more tolerant to motion.

5. CONCLUSIONS

The results from EESTCR show that it is a promising method for reconstructing images from undersampled data without the loss of sharpness of edges that one would expect due to the undersampling of high frequencies in the acquired data. Images reconstructed from 24 rays of k-space were shown to be improved using EESTCR in comparison to current state of the art [8]. EESTCR can be used to improve the sharpness of edges of undersampled data even in the presence of some respiratory motion.

Acknowledgements: This work was supported by R01 EB006155

6. FIGURES

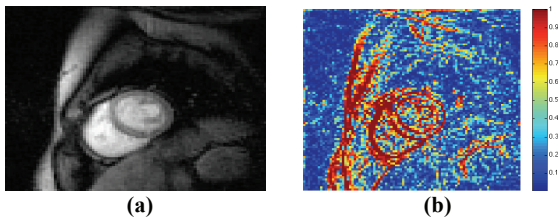


Figure 1. (a) The reference formed by taking the IFT for fully sampled k-space data simulated from Cartesian acquisition. (b) The edge function ω for $\lambda=0.1$. The value of ω is close to 1 for sharp edges and close to 0 over smooth regions.

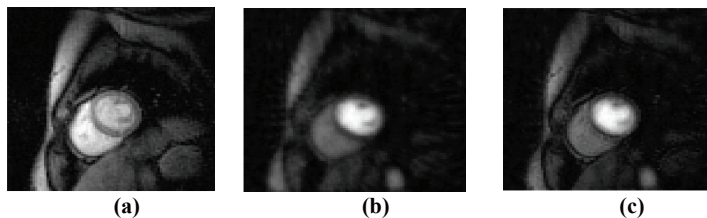


Figure 2. Result of reconstruction from simulated radial acquisition from a single coil using EESTCR, 24 radial lines. (a) Reference image formed by taking the inverse Fourier transform of fully sampled k-space data. (b) Inverse Fourier transform of under-sampled radial data for a single time frame. (c) Reconstructed image using EESTCR. The edges in the reconstructed image are sharper due to the use of the edge enhancement function.

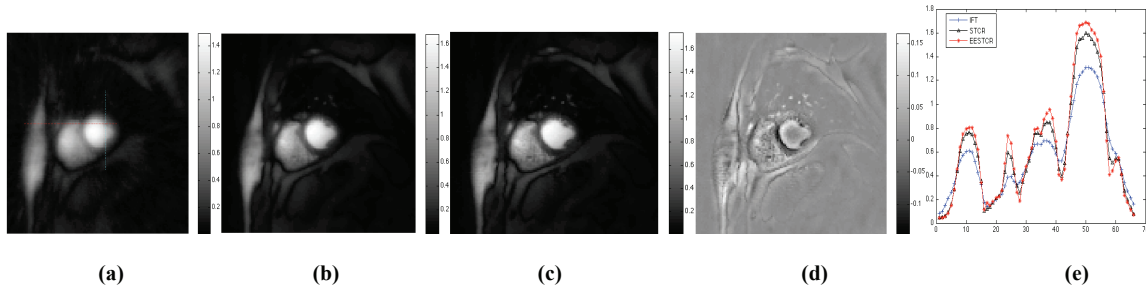


Figure 3. Results of reconstruction from actual radial acquisition (24 rays). One time frame is shown. All reconstructions were done separately on each coil and combined with the square-root-of-sum-of-squares method. (a) Reconstructed without constraints. (b) Reconstructed using STCR. (c) Reconstructed using EESTCR. (d) Difference image formed by taking the difference between reconstruction using EESTCR (c) and STCR (b). The scale shows the percent change. (e) Line profile of no constraints, STCR and EESTCR reconstructed images across the red horizontal line shown faintly in (a). (f) Line profile of no constraints, STCR and EESTCR reconstructed images across the blue vertical line shown faintly in (a). The edges for the image reconstructed using EESTCR were sharper than with STCR and increase in contrast was also seen.

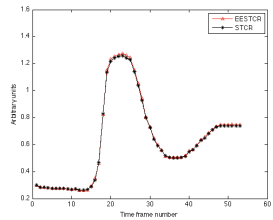
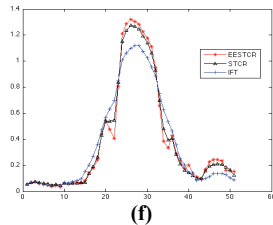


Figure 4. Comparison of mean signal intensity time curves for a small region in the blood pool for images reconstructed using STCR and EESTCR. The curves match well.

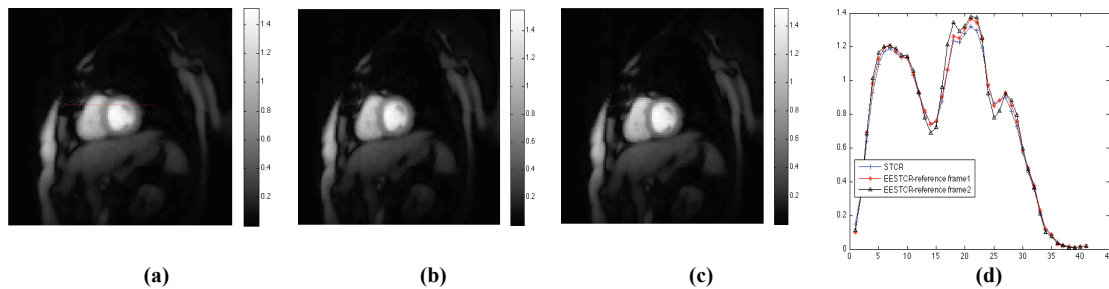


Figure 5. Comparison of reconstructions of another acquired radial dataset (24 rays) with STCR and EESTCR, using two different reference frames. (a) STCR. (b) EESTCR using a reference frame constructed by combining the last 4 frames in the dynamic series. (c) EESTCR using a reference frame constructed by combining 4 frames from the centre of the dynamic series in which there was better contrast. (d) Line profile across the horizontal line shown in (a) for STCR and EESTCR with the two different reference images. Reconstruction using EESTCR with a reference frame constructed by combining 4 frames from the centre of the dynamic sequence provided slightly sharper edges.

7. REFERENCES

- [1] Van Vaals JJ, Brummer ME, Dixon TW, Tuithof HH, Engels H, Nelson C, Gerety BM, Chezmar JL, den Boer JA. Keyhole method for accelerating imaging of contrast agent uptake. *J Magn Reson Imaging* 1993;3:671–675.
- [2] Jones RA, Haraldseth O, Muller TB, Rinck PA, Oksendal AN. k-Space substitution: a novel dynamic imaging technique. *Magn Reson Med* 1993;29:830–834.
- [3] Webb AG, Liang Z-P, Magin RL, Lauterbur PC. Application of reduced encoding MR imaging with generalized-series reconstruction (RIGR). *J Magn Reson Imaging* 1993;3:925–928.
- [4] Hanson JM, Liang Z-P, Wiener EC, Lauterbur PC. Fast dynamic imaging using two reference images. *Magn Reson Med* 1996;36:172–175. 1031-1042, 2003.
- [5] Mistretta CA, Wieben O, Velikina J, Block W, Perry J, Wu Y, Johnson K, Wu Y. Highly constrained backprojection for time-resolved MRI. *Magn Reson Med*. 2006 Jan;55(1):30-40.
- [6] Adluru G, Awate SP, Tasdizen T, Whitaker RT, Dibella EV. Temporally constrained reconstruction of dynamic cardiac perfusion MRI. *Magn Reson Med*. 2007 Jun;57(6):1027-36.
- [7] Adluru G, Whitaker RT, DiBella EVR. Spatio-temporal constrained reconstruction of sparse dynamic contrast enhanced radial MRI data. Proc. 4th IEEE International Symposium on Biomedical Imaging 2007.
- [8] Adluru G, McGann C, Speier P, Kholmovski EG, Shaaban A, Dibella EV. Acquisition and reconstruction of undersampled radial data for myocardial perfusion magnetic resonance imaging. *J Magn Reson Imaging*. 2009 Feb;29(2):466-73.